Journal of Power Sources 476 (2020) 228715

Contents lists available at ScienceDirect

Journal of Power Sources

journal homepage: www.elsevier.com/locate/jpowsour

Chronoamperometry and linear sweep voltammetry reveals the adverse impact of high carbonate buffer concentrations on anode performance in microbial fuel cells

Ruggero Rossi [a], Deepak Pant [b], Bruce E. Logan [a,*]

[a] Department of Civil and Environmental Engineering, The Pennsylvania State University, University Park, PA, 16802, USA
[b] Separation & Conversion Technology, Flemish Institute for Technological Research (VITO), Boeretang 200, Mol, 2400, Belgium

HIGHLIGHTS

- Comparison of maximum power density do not allow evaluating the anode performance.
- Polarization curves should be used in conjunction with anode chronoamperometry.
- Increasing the buffer concentration in MFCs results in a plateau in maximum power.
- Poor anode performance at high buffer concentration were due to solution salinity.
- Cathode and solution resistances decrease with higher buffer concentration.

GRAPHICAL ABSTRACT

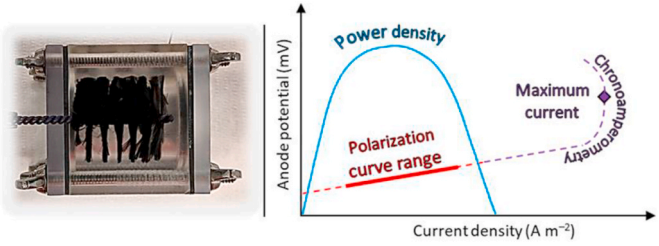

ARTICLE INFO

Keywords:
Chronoamperometry
Carbonate buffer
Phosphate buffer
MFC
Electrode resistance

ABSTRACT

Anode performance in microbial fuel cell (MFC) is usually examined by monitoring anode potentials in whole-cell polarization tests. However, this method does not fully test anode capabilities at higher current densities. To determine maximum anode current densities over a range of carbonate buffer (CB) concentrations we examined electrode performance using chronoamperometry, linear sweep voltammetry (LSV), and electrode potentials during polarization tests. Maximum anode current densities using chronoamperometry at +200 mV reached 42 ± 1 A m^{-2} in 200 mM CB, with lower current densities using 300, 400 mM, or 50 mM CB, consistent with anode LSV data. However, upper current densities were limited to <25 A m^{-2} when analyzed using polarization data due to solution and cathode resistances limiting higher current densities. The maximum power density of 3270 ± 50 mW m^{-2} in 200 mM CB was similar to that obtained with higher buffer concentrations, incorrectly suggesting no adverse impact of higher CB concentrations on anode performance. Analysis using the electrode potential slope (EPS) method showed a clear and measurable unfavorable impact of higher CB concentrations on anode resistances. These results demonstrate that impacts of solution chemistry on anode performance could require current densities higher than those possible using polarization data.

* Corresponding author.
E-mail address: blogan@psu.edu (B.E. Logan).

https://doi.org/10.1016/j.jpowsour.2020.228715
Received 8 April 2020; Received in revised form 30 June 2020; Accepted 30 July 2020

1. Introduction

Microbial fuel cells (MFCs) can generate electrical energy from the biological oxidation of organic compounds in solution [1,2]. Exoelectrogenic microorganisms catalyze the oxidation reaction and release electrons that are then used in the oxygen reduction reaction (ORR) on the cathode, generating an electrical current [3]. Protons are released at the anode and hydroxyl ions at the cathode which can lead to large differences in the local pH between each of the electrodes [4–6]. The protons generated at the anode can acidify the biofilm limiting the maximum current density while the rise of the cathodic pH decreases the potential output of the cell based on the Nernst equation [4–7]. Due to the higher concentration in solution of other charged species such as Na^+, K^+, Cl^-, protons and hydroxyl ions (~0.1 μM) are not primarily transported between the electrodes [5]. Thus, buffers are usually required in MFCs to provide a better control of the pH near the electrodes and in the bulk solution. Phosphate buffer is the most commonly used buffer in MFC studies due to its biocompatibility and pKa close to neutral pH [8,9]However, many other buffers can be used including carbonate, PIPES or HEPES [10–14].

Carbonate buffers have been proposed as a more favorable alternative to phosphate buffers for microbial electrochemical experiments in laboratory studies [15], and it is more relevant to wastewater tests as the buffer capacity of a wastewater is dependent by its bicarbonate alkalinity and not the phosphate ion concentration. However, the impact of carbonate buffers, especially at higher concentrations, has not been well investigated relative to anode or MFC performance compared to phosphate buffers. A carbonate buffer can be better for anode performance and it has higher pKa's than a phosphate buffer. For example, in a number of studies it was suggested through modelling and experimental data, that, due to higher diffusion coefficient of carbonate species compared to phosphate, MFCs fed with carbonate buffer had higher performance than those fed with phosphate buffer [10,11,16]. Carbonate and phosphate buffer pKa's are:

$$HCO_3^- + H_2O \rightleftharpoons H_2CO_3 + OH^- \quad pKa_1 = 6.4 \tag{1}$$

$$CO_3^{2-} + H_2O \rightleftharpoons HCO_3^- + OH^- \quad pKa_2 = 10.3 \tag{2}$$

$$H_3PO_4 + H_2O \rightleftharpoons H_2PO_4^- + H_3O^+ \quad pKa_1 = 2.2 \tag{3}$$

$$H_2PO_4^- + H_2O \rightleftharpoons HPO_4^{2-} + H_3O^+ \quad pKa_2 = 7.2 \tag{4}$$

$$HPO_4^{2-} + H_2O \rightleftharpoons PO_4^{2-} + H_3O^+ \quad pKa_3 = 12.3 \tag{5}$$

As a result of these different pKa's, the performance of the MFC can vary based on the pH and buffer composition. For example, it was shown that at a pH of 7 the power density in 200 mM carbonate buffer was 1948 mW m^{-2}, but at a pH of 9 the maximum power density increased by 42% to 2770 mW m^{-2} while performance in phosphate buffers have usually been shown to peak at neutral pH [10,17,18]. These results suggest that better performance of mixed cultures could be obtained by using a carbonate buffer instead of a phosphate buffer. While it has been shown that increasing phosphate buffer solution (PBS) concentrations up to 200 mM produces the highest maximum power densities, the impact of carbonate buffers has received less attention [1]. The buffer concentration impacts all the components of the MFC, but to date the impact of carbonate buffer has not been examined on the individual anode, cathode, and solution resistances of the MFCs. Each of these resistances contributes to the total internal resistance of the reactor and the analysis of them provide more insightful information on the performance in respect to the maximum power density [19].

To fully evaluate anode performance current densities should be examined that exceed those possible based on polarization data. The performance of electrodes is usually monitored based on measured potentials (versus a reference electrode) during polarization and power density curves by either changing the resistance in the circuit, or changing whole cell voltages using linear sweep voltammetry (LSV). However, using different resistances or whole-cell LSV sweeps does not allow testing of an electrode over a wide range of current densities as current densities will be limited by the total internal resistance of the cell. When evaluating cathode performance, LSVs or chronoamperometry tests are often conducted to measure its performance over a wider range of potentials than those possible in whole-cell polarization tests [7,20]. While separate tests can also be done for anode [7], these additional tests are rarely reported.

In this study we examined the impact of CB concentration on anode performance using three methods to obtain a wide range of current densities: chronoamperometry, LSVs, and potentials in polarization curves. To be able to achieve high current densities we acclimated the anode to a fixed and high anode potential of +200 mV (vs a standard hydrogen electrode, SHE). To achieve the best possible MFC performance in polarization tests, it is necessary to maintain a high anode potential during acclimation to avoid performance limitations due to poor biofilm acclimation [21]. For example, using a potentiostat to maintain high anode potential during acclimation has been shown to increase the abundance of *Geobacter* spp. on the anode (by 8%) in mixed cultures, compared with reactors run at a fixed external resistance after 18 days of operation [22]. By using such a high anode potential, it was therefore possible to better acclimate the anode to current densities higher than those possible due to only changing resistances due to loss of voltage by the internal resistance. Buffer concentrations become critical to anode performance at high current densities in order to avoid low anode pHs. Thus, a carbonate and phosphate buffer could produce different results at high current densities due to their different pKa's, which can lead to different optimal pHs for anode and cathode performance in MFCs [23,24]. By monitoring the current produced at a high positive potential of +200 mV it was possible to determine the impact of carbonate buffer concentrations on the ability of the bioanode to produce high current densities avoiding the detrimental impact of the large cathode overpotential. To compare this approach with more typical methods of analyzing MFC performance based on power density curves, we analyzed polarization data obtained using LSVs with the electrode potential slope (EPS) method to quantify the individual anode and cathode resistances in the different buffer solutions at different concentrations of CB [19,25].

2. Materials and methods

2.1. Construction and operation of MFCs

The MFCs were cubic-shaped reactors constructed from polycarbonate blocks with an inside cylindrical chamber 3 cm in diameter and 4 cm in length. The anodes (5 cm^2 projected area, Mill-Rose, USA) were graphite fiber brushes (2.5 cm in both diameter and length) wound using two titanium wires, heat treated at 450 °C in a furnace for 30 min prior to use, and placed horizontally in the middle of the MFC chamber [26]. Brush anodes were placed perpendicular to the cathode, with a 1 cm space between the electrodes. Cathodes (7 cm^2 projected area) were commercially available electrodes (VITO CORE®, VITO, Mol, Belgium) with a 70% porosity diffusion layer (PTFE) and an activated carbon catalyst pressed on a stainless steel mesh current collector [27]. The MFCs were operated in triplicate at a constant anode potential of +200 mV vs standard hydrogen electrode (SHE) in a temperature-controlled room at 30 °C. The high electrode potential was selected to maximize the anode performance, as previously showed by modelling and experimental studies [28,29]. Despite connecting the MFC to an external resistance was the most common method to acclimate the reactor [26], here the anode electrode was poised at a high potential to avoid the impact of the large cathodic overpotential on the MFC performance and on the anode acclimation. Anodes were inoculated with MFC effluent from other reactors operating for >1 year as previously described [30].

MFCs were fed in batch mode with carbonate buffer at

concentrations of 50 mM (CB_{50}; 0.31 g L^{-1} NH_4Cl, 0.60 g L^{-1} NaH_2PO_4, 0.62 g L^{-1} K_2CO_3, 3.82 g L^{-1} $NaHCO_3$, pH of 8.3, conductivity of 5.2 mS cm^{-1}), 100 mM (CB_{100}; 0.31 g L^{-1} NH_4Cl, 0.60 g L^{-1} NaH_2PO_4, 1.24 g L^{-1} K_2CO_3, 7.6 g L^{-1} $NaHCO_3$, pH of 9.0, conductivity of 9.3 mS cm^{-1}), 200 mM (CB_{200}; 0.31 g L^{-1} NH_4Cl, 0.60 g L^{-1} NaH_2PO_4, 2.49 g L^{-1} K_2CO_3, 15.3 g L^{-1} $NaHCO_3$, pH of 8.9, conductivity of 16.28 mS cm^{-1}), 300 mM (CB_{300}; 0.31 g L^{-1} NH_4Cl, 0.60 g L^{-1} NaH_2PO_4, 3.7 g L^{-1} K_2CO_3, 22.9 g L^{-1} $NaHCO_3$, pH of 9.1, conductivity of 22.2 mS cm^{-1}), or 400 mM (CB_{400}; 0.31 g L^{-1} NH_4Cl, 0.60 g L^{-1} NaH_2PO_4, 5.0 g L^{-1} K_2CO_3, 30.6 g L^{-1} $NaHCO_3$, pH of 9.1, conductivity of 28.5 mS cm^{-1}), with acetate as a substrate for cycle length of ~12 h. The high feeding frequency allowed maintaining a high substrate concentration in the media. The media were amended with 12.5 mL L^{-1} of a concentrated trace mineral solution and 5 mL L^{-1} of a vitamin solution [31]. Even though the addition of osmoprotector such as betaine or ectoine is not feasible for practical applications, a low concentration (5 mM) was added to CB at the highest concentration of 300 mM and 400 mM to investigate the maximum MFC performance while minimizing the impact of the high salinity on the microbial biofilm. When fed with 400 mM CB, betaine or ectoine (5 mM) were added to the solution and with 300 mM CB, 5 mM betaine was added to the solution. The MFCs operated with the anode potential set at + 200 mV vs SHE, with the cathode as the counter electrode, to minimize the impact of the external resistance on the MFC operation [29,32,33].

2.2. Electrochemical measurements

To investigate MFC performance, LSVs were conducted on the anode electrode at a scan rate of 0.1 mV s^{-1} from the open circuit potential (OCP) to +200 mV vs SHE while also measuring the correspondent cathode potential. Prior to the LSVs, the working electrodes were left for 2 h at the OCP and then a fast electrochemical impedance spectroscopy (EIS) spectrum (from 100 kHz to 500 Hz, 5 mV amplitude, 10 points s^{-1}, ≈25 s $scan^{-1}$) was recorded at the OCP to calculate the solution resistance between anode and reference electrode (RE) ($R_{\Omega\text{-AnRE}}$) [34]. At the end of the LSVs, the solution resistance between the RE and the cathode ($R_{\Omega\text{-CatRE}}$) was measured with EIS [34,35]. The reported electrode potentials were corrected based on the solution resistance between each electrode and the RE [34,35]. The measured electrode potentials (not corrected for R_Ω) are reported in the Supporting Information. The RE used to measure the electrode potentials (single junction silver chloride (Ag/AgCl) reference electrode; model RREF0021, Pine Research Instrumentation, NC; + 199 mV versus SHE) was placed in the current path between the electrodes, with the RE tip as close as possible to the brush anode Ti wire [34,35]. Current density (j) and power density (P) were calculated from the current (i) and normalized by the MFC cross-sectional area ($A = 7$ cm^2) [36,37]. All potentials are reported here versus SHE.

The performance of the electrodes was examined using the (EPS) method [19]. For the EPS method it is assumed that there can be a relatively rapid change in the electrode potential due to activation losses at the initial low current densities, and then the electrode potential becomes directly proportional to the current density. Based on these circumstances, the linearized portion of the electrode potential near the peak power density can be used to assess anodic ($E_{An,e0}$) and cathodic ($E_{Cat,e0}$) potentials under the experimental conditions in order to better describe the electrode performance in terms of experimental electrode potentials rather than open circuit potentials. The slopes of the linearized portion of the electrode potentials were used to calculate the anode (R_{An}) and cathode (R_{Cat}) resistances, with the solution resistance (R_Ω) as the third component of the total internal resistance of the cell. Thus, the linearized portion of the electrode potentials from polarization curves in function of the current density was fit to $E = m\,j + b$, where j is the current density, the slope m is defined as the specific resistance of the anode (R_{An}) or cathode (R_{Cat}) in units of mΩ m^2, and the y-intercepts are used to calculate the experimental open circuit potentials of the anode ($E_{An,e0}$) or cathode ($E_{Cat,e0}$) [19].

3. Results and discussion

3.1. Impact of media composition on buffer capacity

With a 50 mM carbonate buffer solution the initial pH was 8.3, higher than that of a typical 50 mM PBS solution (pH = 7.0) (Figure S1). The buffer capacity is defined as the amount of acid or base that can be added to a solution without changing the pH by more than 1 pH unit. The buffer capacity of CB, calculated between pH 7 and 6, was 40 mM pH^{-1}, 38% larger than that of PBS (29 mM pH^{-1}) in the same pH range.

The higher buffer capacity of CB was likely due to the closer pKa of the carbonate ($pKa_1 = 6.4$, $pKa_2 = 10.3$) buffer species compared to phosphate buffer ($pKa_1 = 2.2$, $pKa_2 = 7.2$, $pKa_2 = 12.3$). It was previously reported that the addition of carbonate buffer to the MFC media increased the reactor performance due to the higher diffusivity of HCO_3^- than $H_2PO_4^-$ [10,13,16]. However, we showed here that the higher current and power densities in carbonate buffer fed systems compared to those previously obtained in phosphate buffer fed reactors were likely due to the higher buffer capacity of CB than PBS, and not the higher diffusivity of bicarbonate than monophasic phosphate in solution.

3.2. Maximum current densities from chronoamperometry as a function of CB concentration

Increasing the carbonate buffer concentration from 50 mM to 200 mM produced larger current densities with brush anodes polarized at +200 mV vs SHE (Fig. 1). The anodes showed relatively stable performance in 50 mM CB 21 days after inoculation, with maximum current densities of 22 ± 1 A m^{-2} (26 d). Doubling the buffer concentration to 100 mM increased the maximum current density by 32%, to 29 ± 2 A m^{-2} (42 d), and using 200 mM buffer further increased the current by 41%, to 41 ± 2 A m^{-2} (68 d) relative to that in the 100 mM buffer.

To investigate if the maximum current in chronoamperometry was limited to the substrate depletion or to the buffer capacity of the media, the acetate concentration in 200 mM CB was increased from 2 g L^{-1} to 4 g L^{-1} from day 52 to day 54. The anode performance was not affected by the acetate concentration as the average maximum current density was 37 ± 1 A m^{-2} compared to 36 ± 2 A m^{-2} obtained with 2 g L^{-1} acetate. The impact of the cycle length on the anode performance was investigated by feeding the MFC every 24 h instead of 12 h and maintaining the same acetate supply to the anode (4 g L^{-1}). The maximum current density decreased by feeding the reactors less often. This decreased performance was likely due to the combination of a faster substrate depletion by the microbial community with a highly saline environment (CB_{200} σ = 16 mS cm^{-1}) due to a higher average current density [38]. For example, the maximum current density decreased from 39 ± 1 A m^{-2} with a 12 h cycle length (55 d) to 22 ± 1 A m^{-2} with a 24 h cycle length (56 d). The anode maximum current density returned to 37 ± 2 A m^{-2} after one week of continuous operation by feeding the reactors every 12 h.

Higher CB concentrations of 300 or 400 mM decreased the anode performance, as shown by the decrease in the anode maximum current density, likely due to the high salinity of the solution that has previously been shown to negatively affect biofilm performance [39]. Feeding the MFCs with 400 mM CB immediately reduced the maximum current density to 35 ± 1 A m^{-2}, and further reduced to 9 ± 2 A m^{-2} after one week, and to only 3 ± 1 A m^{-2} after nine days of operation. Adding osmoprotectors such as ectoine or betaine did not improve anode

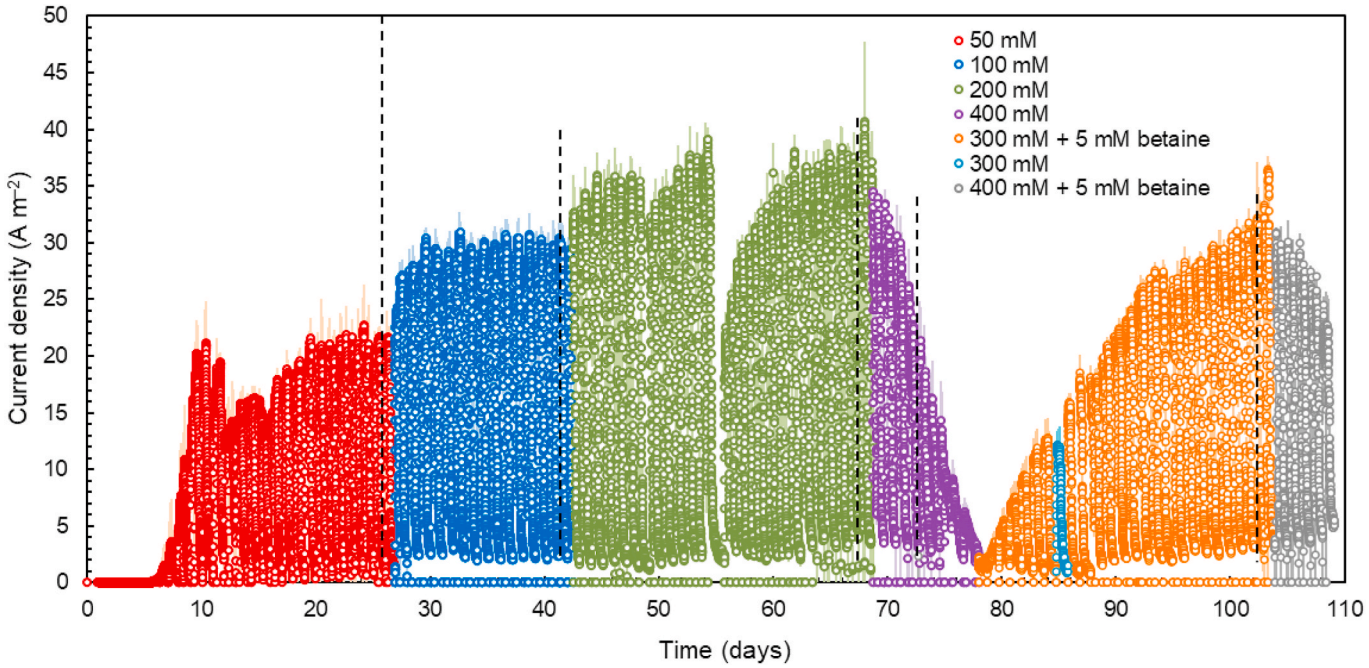

Fig. 1. Chronoamperometry of the brush anodes (set at +200 mV) using different carbonate buffer concentrations. Dashed lines indicate when polarization tests were performed. The decrease in current over each cycle (~0.5 d) resulted from substrate depletion in the medium. For one cycle betaine was removed from the 300 mM CB, as showed by the light blue color at day 87. (For interpretation of the references to color in this figure legend, the reader is referred to the Web version of this article.)

performance for these MFCs at a set anode potential of 200 mV, contrary to that found in a previous study [40]. In that study using a mixed culture dominated by *Acinetobacter*, the authors found a 60% increase in performance based on the average voltage after adding ectoine (up to 517 mM NaCl, or 30 g L^{-1}), although their results were obtained using a 1000 Ω external resistance rather than a set anode potential [40]. Slightly decreasing the CB concentration to 300 mM in presence of betaine partially restored the anode performance, producing a maximum current density of 30 ± 1 A m^{-2} (106 d). Despite the large decrease in current densities produced by using 400 mM CB, there was a gradual recovery of the anode performance in 300 mM CB in the presence of betaine. Removing the betaine from the media (84 d Fig. 1) during acclimation limited the performance recovery decreasing the maximum anode current density, from 12 ± 1 A m^{-2} to 10 ± 1 A m^{-2}. Reintroducing betaine in solution the following cycle increased the current density to 19 ± 2 A m^{-2}. To examine whether operation using 300 mM buffer might have better acclimated the biofilm to higher buffer concentrations the buffer concentration was again increased to 400 mM but this resulted once more in unstable performance (Fig. 1). Inoculation of new brushes using 300 mM CB with or without betaine also did not produce any appreciable current density (Figure S3). These results suggested that betaine was effective in improving current generation only of an existing biofilm and that its addition did not favor the acclimation of microorganisms on a new electrode in a higher concentration buffer solution.

3.3. Maximum power densities from LSVs as a function of CB concentration

To compare the impact of CB concentration observed using a high set anode potential with more traditional methods based on power density curves, we obtained polarization data using LSVs. Following multiple cycles of acclimation to each different buffer concentration, polarization data were obtained at the indicated times shown in Fig. 1, and then the MFCs were returned to operation at a set potential. Maximum current densities in polarization tests were always lower than that obtained from fixed anode potential, for all buffer concentration tested here (Fig. 2A). For example, the maximum current density was 22 ± 1 A m^{-2} (50 mM CB) and 41 ± 2 A m^{-2} (200 mM CB) in chronoamperometry but decreased to 9.6 ± 0.7 A m^{-2} (50 mM CB) and 24 ± 1 A m^{-2} (200 mM CB) in power density tests. These lower current densities were a consequence of the decrease in cathode potential and whole cell potential that did not allow to reach higher current densities in the range that was possible in chronoamperometry tests.

Increasing the CB concentration showed a beneficial impact of using more conductive solutions, based on the decreased in the internal resistance calculated from the slope of the polarization curves, except for the 300 mM CB solution. For example, R_{int} decreased from 58.6 ± 0.4 mΩ m^2 (50 mM CB) to 25.5 ± 0.1 mΩ m^2 (200 mM CB) consistent with the anode performance from chronoamperometric results. However, the internal resistance did not appreciably decrease in the higher buffer concentration solutions (23.7 ± 0.1 mΩ m^2, 300 mM CB; and 22.5 ± 0.1 mΩ m^2, 400 mM CB). In addition, the maximum current density based on the x-intercept at high current densities was similar for the 200 mM CB (24 ± 1 A m^{-2}) and the 300 mM CB (24 ± 2 A m^{-2}), although it was reduced to 20 ± 2 A m^{-2} in 400 mM CB. The OCP was not affected by the CB concentration and averaged 656 ± 14 mV over all these experiments.

Based on the maximum power density from MFCs, there was no adverse impact on the performance of using CB concentrations of 300 mM and 400 mM, in contrast with the results obtained from the chronoamperometry tests. Increasing the CB concentration showed beneficial impact on the MFC whole cell performance at all buffer concentrations tested, with maximum power densities 64% larger with 100 mM CB (2080 ± 80 mW m^{-2}) than that obtained using 50 mM CB (1270 ± 80 mW m^{-2}) (Fig. 2B). Further increasing the CB concentration to 200 mM produced an additional 58% increase in the maximum power density (3270 ± 50 mW m^{-2}). Higher buffer concentrations did not further improve or adversely impact MFC performance based on polarization data, with maximum power densities similar to that obtained with 200 mM CB, 300 mM (3190 ± 150 mW m^{-2}) and 400 mM CB (3330 ± 290 mW m^{-2} on day 74).

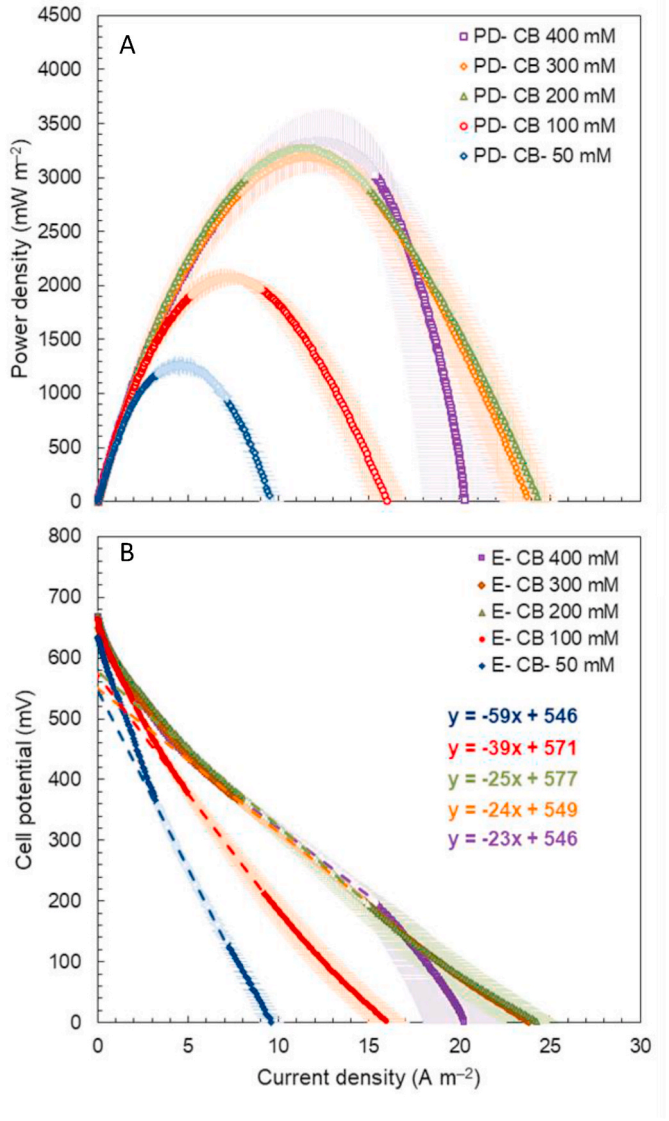

Fig. 2. (A) Power density curves and (B) polarization curves from LSVs of MFCs fed with different carbonate buffer concentrations. The dashed lines represent the linearization of the data from polarization tests used to calculate the MFC internal resistance (R_{int}).

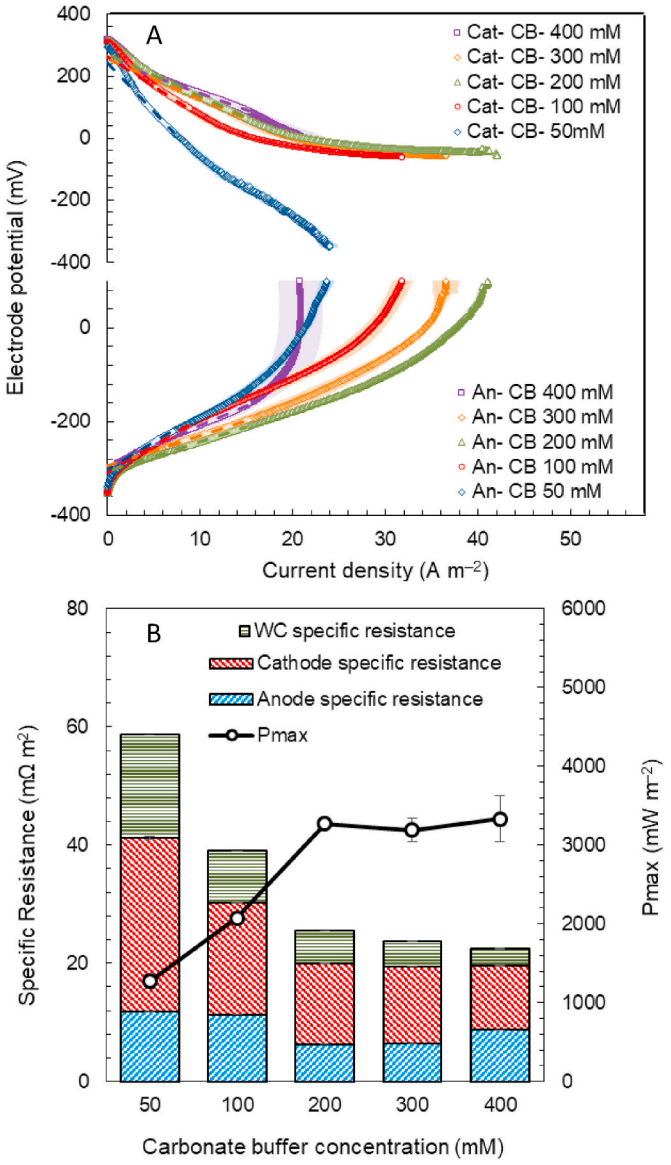

Fig. 3. (A) Cathode (Cat) and anode (An) potentials from polarization tests following correction for ohmic resistance. The dashed lines represent the linearization of the data that would be obtained from polarization tests, while the thick solid lines show the linearized portion of the slopes that are used to calculate the anode (R_{An}) and cathode (R_{Cat}) resistances. Electrode potentials not corrected for ohmic losses are reported in the Supporting information. (B) Comparison of the electrode resistances and the correspondent maximum power density in different carbonate buffer concentrations.

The similar overall performance of the MFCs at the higher buffer concentrations was unexpected given the clear adverse impact of the higher CB concentrations on anode performance in terms of measured current densities at a set anode potential of +200 mV (Fig. 1). This lack of a change in overall power production suggested that there were other factors that impacted overall performance, likely due to the different current density range in the two experiments. For example, the current density at the maximum power density in 50 mM CB was 4.6 ± 0.2 A m^{-2}, much lower than the maximum current density obtained when anode potential was set at +200 mV (22 ± 1 A m^{-2}).

3.4. Analysis of electrode resistances using the EPS method

The EPS analysis conducted on the electrode potentials where the maximum power density occurs, showed that R_{Cat} was the main contributor to R_{int} in all the media tested here, and that increasing the CB concentration impacted the electrodes and the solution resistances to different extents (Fig. 3). The solution resistance and the cathode resistance continuously decreased by increasing the CB concentration while the anode resistance was at a minimum with CB 200 mM, and then it increased in the higher CB concentrations. The trend in R_{An} with CB concentration was in agreement with results based on the anode maximum current densities obtained with the anode potential fixed at +200 mV. For example, R_{An} decreased from 50 mM (11.7 ± 0.1 mΩ m^2) to 200 mM (6.3 ± 0.0 mΩ m^2), but it increased back with 300 mM (6.4 ± 0.0 mΩ m^2) and 400 mM (8.7 ± 0.0 mΩ m^2) CB solutions. These changes in resistance were relatively small compared to the sum of $R_{Cat} + R_{\Omega}$, thus resulting in similar R_{int} for CB > 200 mM and similar maximum power densities. For example, $R_{\Omega} + R_{Cat}$ was 46.9 ± 0.4 mΩ m^2 with 50 mM CB, and decreased to 13.9 ± 0.1 mΩ m^2 with 400 mM CB. The largest change in the individual resistance was in R_{Cat}, decreasing by 66% from 50 mM to 200 mM CB, with no change of $E_{Cat,e0}$ (257 ± 9 mV) likely due to a shift in the ORR pathways, that have been showed to be strongly affected by the local pH [41].

3.5. Comparison of performance of MFCs fed using CB with previous PBS studies

The maximum power densities obtained here in CB are slightly lower than those previously reported with similar MFC configuration fed with PBS [19]. For example, maximum power densities here in 50 mM CB was $P_{max50} = 1270 \pm 80$ mW m^{-2}, compared to 1710 ± 80 mW m^{-2} in 50 mM PBS [19], and in CB 200 mM was $P_{max200} = 3270 \pm 50$ mW m^{-2} compared to 3420 ± 80 mW m^{-2} in 200 mM PBS [42] (all tests with an activated carbon cathode and brush anode, and similar electrode spacing). However, by using the EPS analysis it was possible to identify how the individual electrodes contributed to the overall performances in these studies. For example, the cathode overpotential was responsible here for the lower maximum power density in 50 mM CB with respect to that reported in 50 mM PBS, not the anode. This reduced performance of the cathode in CB was likely due to the ORR kinetics being adversely impacted by higher pHs, with the cathode resistance doubling in CB 50 mM at pH 8.4 ($R_{Cat} = 31.7 \pm 0.3$ mΩ m^2) compared to that previously reported in 50 mM PBS at pH 7 ($R_{Cat} = 14.8 \pm 0.9$ mΩ m^2) [19]. The cathode experimental potentials were not a factor as they were similar in the two media (50 mM CB, $E_{Cat,e0} = 247 \pm 1$ mV; 50 mM PBS, $E_{Cat,e0} = 243 \pm 2$ mV), despite predicted differences of a lower potential of 83 mV at the higher pH using the Nernst equation. The anode in 50 mM CB showed improved performance with a 43 mV lower experimental potential ($E_{An,e0} = -303 \pm 1$ mV) compared to that previously reported using a 50 mM PBS ($E_{An,e0} = -260 \pm 3$ mV). This lower potential was likely due to the higher pH of the CB than that of the PBS as the anode resistances were similar in the two different electrolytes (50 mM CB, $R_{An} = 11.7 \pm 0.1$ mΩ m^2; 50 mM PBS, $R_{An} = 10.6 \pm 0.5$ mΩ m^2). While the use of a high set anode potential was needed to test the limits of performance of the electrode in the different CB solutions, the EPS method was therefore helpful in distinguishing the specific factors that impacted performance such as the electrode potentials and resistances.

4. Conclusions

Comparisons of anode performance in MFCs requires direct measurement of the anode potentials rather than just a comparison based on maximum power densities. It was shown here using different CB concentrations that power density curves did not reveal differences in anode performance for CB concentrations larger than 200 mM. However, by using a high and fixed anode potential it was possible to identify a large impact of the CB concentration on the anode performance based on showing that the maximum current density decreased from 41 ± 2 A m^{-2} in 200 mM CB, to 30 ± 1 A m^{-2} in 300 mM CB, and to only 3 ± 1 A m^{-2} after nine days of operation with 400 mM CB. Similar maximum power densities with CB concentrations >200 mM were due to increases in the anode resistances (R_{An}) being offset by decreases in the cathode and solution resistances ($R_{Cat} + R_{\Omega}$) with higher CB concentrations, thus resulting in a relatively unchanged overall internal resistance. These results show that maintaining a high anode potential during MFC operation can allow for direct measurements of the impact of solution conditions such as electrolytes having different pHs, conductivities, and buffer strength.

Author contribution

All authors researched data, wrote the article, and reviewed and edited the manuscript before submission.

Declaration of competing interest

The authors declare that they have no known competing financial interests or personal relationships that could have appeared to influence the work reported in this paper.

Acknowledgements

The authors acknowledge funding by the Environmental Security Technology Certification Program via cooperative research agreement W9132T-16-2-0014 through the US Army Engineer Research and Development Center.

Appendix A. Supplementary data

Supplementary data to this article can be found online at https://doi.org/10.1016/j.jpowsour.2020.228715.

References

[1] B.E. Logan, R. Rossi, A. Ragab, P.E. Saikaly, Electroactive microorganisms in bioelectrochemical systems, Nat. Rev. Microbiol. 17 (2019) 307–319, https://doi.org/10.1038/s41579-019-0173-x.
[2] B.E. Logan, Exoelectrogenic bacteria that power microbial fuel cells, Nat. Rev. Microbiol. 7 (2009) 375–381, https://doi.org/10.1038/nrmicro2113.
[3] A. Kumar, L.H.H. Hsu, P. Kavanagh, F. Barrière, P.N.L. Lens, L. Lapinsonnière, J. H. Lienhard, U. Schröder, X. Jiang, D. Leech, The ins and outs of microorganism-electrode electron transfer reactions, Nat. Rev. Chem. 1 (2017) 1–13, https://doi.org/10.1108/10662240210438434.
[4] C.I. Torres, A.K. Marcus, B.E. Rittmann, Proton transport inside the biofilm limits electrical current generation by anode-respiring bacteria, Biotechnol. Bioeng. 100 (2008) 872–881, https://doi.org/10.1002/bit.21821.
[5] S.C. Popat, C.I. Torres, Critical transport rates that limit the performance of microbial electrochemistry technologies, Bioresour. Technol. 215 (2016) 265–273, https://doi.org/10.1016/j.biortech.2016.04.136.
[6] S.C. Popat, D. Ki, B.E. Rittmann, C.I. Torres, Importance of OH^- transport from cathodes in microbial fuel cells, ChemSusChem 5 (2012) 1071–1079, https://doi.org/10.1002/cssc.201100777.
[7] R. Rossi, D.M. Hall, X. Wang, J.M. Regan, B.E. Logan, Quantifying the factors limiting performance and rates in microbial fuel cells using the electrode potential slope analysis combined with electrical impedance spectroscopy, Electrochim. Acta 348 (2020) 136330, https://doi.org/10.1016/j.electacta.2020.136330.
[8] S.C. Popat, D. Ki, M.N. Young, B.E. Rittmann, C.I. Torres, Buffer pKa and transport govern the concentration overpotential in electrochemical oxygen reduction at neutral pH, ChemElectroChem 1 (2014) 1909–1915, https://doi.org/10.1002/celc.201402058.
[9] Y. Ye, X. Zhu, B.E. Logan, Effect of buffer charge on performance of air-cathodes used in microbial fuel cells, Electrochim. Acta 194 (2016) 441–447, https://doi.org/10.1016/j.electacta.2016.02.095.
[10] Y. Fan, H. Hu, H. Liu, Sustainable power generation in microbial fuel cells using bicarbonate buffer and proton transfer mechanisms, Environ. Sci. Technol. 41 (2007) 8154–8158, https://doi.org/10.1038/am.2014.1.
[11] C.I. Torres, H.S. Lee, B.E. Rittmann, Carbonate species as OH^- carriers for decreasing the pH gradient between cathode and anode in biological fuel cells, Environ. Sci. Technol. 42 (2008) 8773–8777, https://doi.org/10.1021/es8019353.
[12] J.J. Fornero, M. Rosenbaum, M.A. Cotta, L.T. Angenent, Carbon dioxide addition to microbial fuel cell cathodes maintains sustainable catholyte pH and improves anolyte pH, alkalinity, and conductivity, Environ. Sci. Technol. 44 (2010) 2728–2734, https://doi.org/10.1021/es9031985.
[13] A.K. Marcus, C.I. Torres, B.E. Rittmann, Evaluating the impacts of migration in the biofilm anode using the model PCBIOFILM, Electrochim. Acta 55 (2010) 6964–6972, https://doi.org/10.1016/j.electacta.2010.06.061.
[14] J.Y. Nam, H.W. Kim, K.H. Lim, H.S. Shin, B.E. Logan, Variation of power generation at different buffer types and conductivities in single chamber microbial fuel cells, Biosens. Bioelectron. 25 (2010) 1155–1159, https://doi.org/10.1016/j.bios.2009.10.005.
[15] B.E. Rittmann, Ironies in microbial electrochemistry, J. Environ. Eng. 143 (2017), 03117001, https://doi.org/10.1061/(ASCE)EE.1943-7870.0001202.
[16] A.K. Marcus, C.I. Torres, B.E. Rittmann, Analysis of a microbial electrochemical cell using the proton condition in biofilm (PCBIOFILM) model, Bioresour. Technol. 102 (2011) 253–262, https://doi.org/10.1016/j.biortech.2010.03.100.
[17] Z. He, Y. Huang, A.K. Manohar, F. Mansfeld, Effect of electrolyte pH on the rate of the anodic and cathodic reactions in an air-cathode microbial fuel cell, Bioelectrochemistry 74 (2008) 78–82, https://doi.org/10.1016/j.bioelechem.2008.07.007.
[18] S. Jung, M.M. Mench, J.M. Regan, Impedance characteristics and polarization behavior of a microbial fuel cell in response to short-term changes in medium pH, Environ. Sci. Technol. 45 (2011) 9069–9074, https://doi.org/10.1021/es201737g.
[19] R. Rossi, B.P. Cario, C. Santoro, W. Yang, P.E. Saikaly, B.E. Logan, Evaluation of electrode and solution area-based resistances enables quantitative comparisons of factors impacting microbial fuel cell performance, Environ. Sci. Technol. 53 (2019) 3977–3986, https://doi.org/10.1021/acs.est.8b06004.
[20] F. Yin, P. Hu, C. Song, S. Wang, H. Liu, Unveiling the role of gas permeability in air cathodes and performance enhancement by waterproof membrane fabricating method, J. Power Sources 449 (2020) 227570, https://doi.org/10.1016/j.jpowsour.2019.227570.
[21] X. Zhu, J.C. Tokash, Y. Hong, B.E. Logan, Controlling the occurrence of power overshoot by adapting microbial fuel cells to high anode potentials,

Bioelectrochemistry 90 (2013) 30–35, https://doi.org/10.1016/j.bioelechem.2012.10.004.
[22] H. Yan, M.D. Yates, J.M. Regan, Effects of constant or dynamic low anode potentials on microbial community development in bioelectrochemical systems, Appl. Microbiol. Biotechnol. 99 (2015) 9319–9329, https://doi.org/10.1007/s00253-015-6907-4.
[23] Z.A. Stoll, J. Dolfing, J. Ren, P. Xu, Interplay of anode , cathode , and current in microbial fuel cells : implications for wastewater treatment, Energy Technol. 4 (2016) 583–592, https://doi.org/10.1002/ente.201500397.
[24] S. Ou, H. Kashima, D.S. Aaron, J.M. Regan, M.M. Mench, Full cell simulation and the evaluation of the buffer system on air-cathode microbial fuel cell, J. Power Sources 347 (2017) 159–169, https://doi.org/10.1016/j.jpowsour.2017.02.031.
[25] B.P. Cario, R. Rossi, K.Y. Kim, B.E. Logan, Applying the electrode potential slope method as a tool to quantitatively evaluate the performance of individual microbial electrolysis cell components, Bioresour. Technol. 287 (2019) 121418, https://doi.org/10.1016/j.biortech.2019.121418.
[26] W. Yang, K.Y. Kim, P.E. Saikaly, B.E. Logan, The impact of new cathode materials relative to baseline performance of microbial fuel cells all with the same architecture and solution chemistry, Energy Environ. Sci. 10 (2017) 1025–1033, https://doi.org/10.1039/c7ee00910k.
[27] F. Zhang, S. Cheng, D. Pant, G. Van Bogaert, B.E. Logan, Power generation using an activated carbon and metal mesh cathode in a microbial fuel cell, Electrochem. Commun. 11 (2009) 2177–2179, https://doi.org/10.1016/j.elecom.2009.09.024.
[28] X. Zhu, M.D. Yates, B.E. Logan, Set potential regulation reveals additional oxidation peaks of Geobacter sulfurreducens anodic biofilms, Electrochem. Commun. 22 (2012) 116–119, https://doi.org/10.1016/j.elecom.2012.06.013.
[29] B. Korth, F. Harnisch, Spotlight on the energy harvest of electroactive microorganisms: the impact of the applied anode potential, Front. Microbiol. 10 (2019) 1–9, https://doi.org/10.3389/fmicb.2019.01352.
[30] G. Liu, M.D. Yates, S. Cheng, D.F. Call, D. Sun, B.E. Logan, Examination of microbial fuel cell start-up times with domestic wastewater and additional amendments, Bioresour. Technol. 102 (2011) 7301–7306, https://doi.org/10.1016/j.biortech.2011.04.087.
[31] S. Cheng, D. Xing, D.F. Call, B.E. Logan, Direct biological conversion of electrical current into methane by electromethanogenesis, Environ. Sci. Technol. 43 (2009) 3953–3958, https://doi.org/10.1021/es803531g.
[32] Y. Hong, D.F. Call, C.M. Werner, B.E. Logan, Adaptation to high current using low external resistances eliminates power overshoot in microbial fuel cells, Biosens. Bioelectron. 28 (2011) 71–76, https://doi.org/10.1016/j.bios.2011.06.045.
[33] V.J. Watson, B.E. Logan, Analysis of polarization methods for elimination of power overshoot in microbial fuel cells, Electrochem. Commun. 13 (2011) 54–56, https://doi.org/10.1016/j.elecom.2010.11.011.
[34] B.E. Logan, E. Zikmund, W. Yang, R. Rossi, K.-Y. Kim, P.E. Saikaly, F. Zhang, Impact of ohmic resistance on measured electrode potentials and maximum power production in microbial fuel cells, Environ. Sci. Technol. 52 (2018) 8977–8985, https://doi.org/10.1021/acs.est.8b02055.
[35] F. Zhang, J. Liu, I. Ivanov, M.C. Hatzell, W. Yang, Y. Ahn, B.E. Logan, Reference and counter electrode positions affect electrochemical characterization of bioanodes in different bioelectrochemical systems, Biotechnol. Bioeng. 111 (2014) 1931–1939, https://doi.org/10.1002/bit.25253.
[36] R. Rossi, B.E. Logan, Unraveling the contributions of internal resistance components in two-chamber microbial fuel cells using the electrode potential slope analysis, Electrochim. Acta 348 (2020) 136291, https://doi.org/10.1016/j.electacta.2020.136291.
[37] L. Lu, J. Gu, Z.J. Ren, Comment on "Unbiased solar H_2 production with current density up to 23 mA cm^{-2} by Swiss-cheese black Si coupled with wastewater bioanode, Energy Environ. Sci. 12 (2019) 3412–3414, https://doi.org/10.1039/c9ee02592h.
[38] F. Zeng, Y. Wu, L. Bo, L. Zhang, W. Liu, Y. Zhu, Coupling of electricity generation and denitrification in three-phase single-chamber MFCs in high-salt conditions, Bioelectrochemistry 133 (2020) 1–9, https://doi.org/10.1016/j.bioelechem.2020.107481.
[39] D. Sun, A. Wang, S. Cheng, M. Yates, B.E. Logan, Geobacter anodireducens sp. nov., an exoelectrogenic microbe in bioelectrochemical systems, Int. J. Syst. Evol. Microbiol. 64 (2014) 3485–3491, https://doi.org/10.1099/ijs.0.061598-0.
[40] F.X. Tan, L.H. Zhang, W.F. Liu, Y.M. Zhu, Osmotic pressure compensated solute ectoine improves salt tolerance of microbial cells in microbial fuel cells, Fuel Cell. 19 (2019) 616–622, https://doi.org/10.1002/fuce.201900051.
[41] S. Rojas-Carbonell, K. Artyushkova, A. Serov, C. Santoro, I. Matanovic, P. Atanassov, Effect of pH on the activity of platinum group metal-free catalysts in oxygen reduction reaction, ACS Catal. 8 (2018) 3041–3053, https://doi.org/10.1021/acscatal.7b03991.
[42] W. Yang, B.E. Logan, Immobilization of a metal-nitrogen-carbon catalyst on activated carbon with enhanced cathode performance in microbial fuel cells, ChemSusChem 9 (2016) 2226–2232, https://doi.org/10.1002/cssc.201600573.